

Polaronic neutron in dilute alpha matter: A p -wave Bose polaron

Hiroyuki Tajima,^{1,2} Hajime Moriya,³ Tomoya Naito,^{4,1} Wataru Horiuchi,^{5,6,2,7} Eiji Nakano,⁸ and Kei Iida^{8,2}

¹*Department of Physics, Graduate School of Science,
The University of Tokyo, Tokyo 113-0033, Japan*

²*RIKEN Nishina Center, Wako 351-0198, Japan*

³*Research Center for Nuclear Physics, Osaka University, Ibaraki, Osaka 567-0047, Japan*

⁴*Interdisciplinary Theoretical and Mathematical Science Program (iTHEMS), RIKEN, Saitama 351-0198, Japan*

⁵*Department of Physics, Osaka Metropolitan University, Osaka 558-8585, Japan*

⁶*Nambu Yoichiro Institute of Theoretical and Experimental Physics (NITEP),
Osaka Metropolitan University, Osaka 558-8585, Japan*

⁷*Department of Physics, Hokkaido University, Sapporo 060-0810, Japan*

⁸*Department of Mathematics and Physics, Kochi University, Kochi 780-8520, Japan*

We theoretically investigate quasiparticle properties of a neutron immersed in an alpha condensate, which is one of the possible states of dilute symmetric nuclear matter. The resonant p -wave neutron-alpha scattering, which plays a crucial role in forming halo nuclei, is considered. This system is similar to a Bose polaron near the p -wave Feshbach resonance that can be realized in cold-atomic experiments. Calculating the low-momentum self-energy within the field-theoretical approach, we give an analytical formula for the effective mass of a polaronic neutron as a function of alpha condensation density. Two adjacent neutrons in a medium, each of which behaves like a stable polaron having an enhanced effective mass, can form a bound dineutron, with the help of 1S_0 neutron-neutron attraction. This is in contrast to the case of the vacuum, where a dineutron is known to be unbound. Moreover, adding an impurity-like neutron to symmetric nuclear matter can be regarded as a perturbation accompanied by an explicit breaking of Wigner's $SU(4)$ symmetry. The relationship between the polaron energy and the Wigner term in nuclear mass formulas is discussed in the low-density limit. Our result would be useful for understanding many-body physics in astrophysical environments as well as the formation of multi-nucleon clusters in neutron-halo nuclei.

I. INTRODUCTION

Infinite symmetric nuclear matter, where the proton charge is switched off, is fictitious, but is one of the most fundamental nuclear systems because it is related to saturation of the binding energy and density of stable nuclei [1]. It is still interesting to consider infinite symmetric nuclear matter at relatively low densities, although naively the system undergoes an instability towards inhomogeneous phases at sufficiently low temperature [2]. Once the proton charge is switched on, the nuclear liquid has to be a collection of nuclei. Furthermore, such symmetric matter can contain alpha particles via alpha clustering; indeed, some medium-heavy symmetric nuclei are predicted to be unstable with respect to alpha decay [3].

The nuclear equation of state and the composition in nuclear statistical equilibrium are important keys to understanding the mechanism of supernova explosions [4] and the dynamics of intermediate-energy heavy-ion collisions. To this end, dilute alpha matter and its Bose-Einstein condensation (BEC) phase have been studied as a good reference system for supernova matter at finite temperatures [5–8]. Alpha particles in such an astrophysical environment play a pivotal role in nucleosynthesis, e.g., triple-alpha reaction via the Hoyle state [9]. Moreover, the alpha condensates have also been discussed in the context of excited states of atomic nuclei [10, 11], which are expected to be present in intermediate energy heavy-ion collisions. However, the many-nucleon and dy-

namical nature of the systems of interest here leads to a lot of uncertainties and model dependencies.

To explore the aforementioned alpha clustering properties more clearly, various low-energy nuclear experiments have been performed. The existence of the alpha condensates has been examined experimentally such as ^{16}O [12] and ^{20}Ne [13]. In addition, experimental explorations of multi-neutron clusters in nuclei of large neutron excess are ongoing [14–17]. While the existence of the tetra-neutron resonance has been discussed based on few-body calculations with multi-nucleon interactions [18–20] (see also a review [21]), it is known that the neutron-nucleus interaction plays a crucial role in the formation of halo nuclei [22]. There are several examples of two-neutron halo nuclei, ^6He [23], ^{11}Li [24], ^{14}Be [25], ^{19}B [26], ^{22}C [27–30], and ^{29}F [31, 32]. Moreover, a recent experiment indicates that dineutron correlations play a crucial role in understanding the cluster structure of ^8He [33, 34]. In between, neutrons and alpha clusters are expected to coexist; alpha clusters in a neutron-skin region of stable tin isotopes with small neutron excess have just recently been identified by a knockout experiment [35].

Generally, to understand how the properties of an impurity particle change in medium from those in vacuum, the notion of a polaron, which was originally proposed to see the properties of mobile electrons in ionic lattices [36, 37], is useful. This is the case with nuclear systems in which the medium and impurity particles can be single nucleons or nucleon composites (nuclear clus-

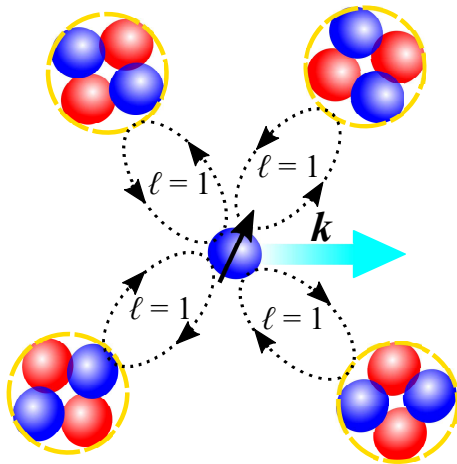


FIG. 1. Schematic picture of a polaronic neutron moving with momentum \mathbf{k} in an alpha condensate, which is characterized by the neutron-alpha $J^\pi = 3/2^-$ p -wave resonance (i.e., relative angular momentum $\ell = 1$).

ters). Polarons are now one of the hot topics in cold atomic physics because of its tunable setup in recent experiments [38]. Some of the present authors clarified the quasiparticle properties of impurity protons and alpha particles in dilute neutron matter as encountered in the crust of a neutron star, in terms of Fermi polarons (i.e., impurities immersed in a Fermi sea) [39–42]. In this regard, it is interesting to consider how neutrons are affected by alpha matter as shown in Fig. 1, which can be relevant to intermediate energy heavy-ion collisions, stellar collapse, and the neutron-skin region of atomic nuclei. Indeed, a similar situation, that is, an impurity surrounded by BEC, is realized in cold-atomic systems as a so-called Bose polaron. Accordingly, the microscopic properties of Bose polarons have been extensively studied experimentally [43–46] and theoretically [47–55] (see also a review [56]).

Another interesting viewpoint on a single impurity-like neutron immersed in alpha matter is that it can probe an explicit breaking of Wigner’s $SU(4)$ symmetry [57–59] because alpha matter can be regarded as an approximately $SU(4)$ symmetric system. Such a response with respect to the neutron addition to $SU(4)$ symmetric matter can be an alternative route for understanding a microscopic origin of the Wigner term that is proportional to the difference between neutron and proton numbers $|N - Z|$ in nuclear mass formula, which was extensively discussed in connection with isoscalar neutron-proton pairing [60]. The relationship between the $SU(4)$ symmetry and the light-cluster formation has also been discussed in the literature [61, 62].

In this paper, we theoretically investigate the quasiparticle properties of a neutron immersed in the alpha condensation state of dilute symmetric nuclear matter, as schematically depicted in Fig. 1. We focus on the resonant $J^\pi = 3/2^-$ p -wave neutron-alpha coupling, which

is responsible for the halo structure of neutron-rich nuclei such as ${}^6\text{He}$ [22]. In this regard, the system we are interested in is similar to Bose polarons near the p -wave Feshbach resonance, which would be experimentally accessible in several Bose-Fermi mixtures (e.g., ${}^6\text{Li}$ - ${}^{87}\text{Rb}$ [63], ${}^{40}\text{K}$ - ${}^{41}\text{K}$ [64], ${}^{23}\text{Na}$ - ${}^{40}\text{K}$ [65], and ${}^6\text{Li}$ - ${}^{133}\text{Cs}$ [66]). This system is different from the one treated in the previous work on polaronic neutrons in spin-polarized neutron matter [67–69]. While p -wave Fermi polarons have been investigated theoretically [70, 71], its bosonic counterpart has yet to be addressed. It is still noteworthy that recently, the role of interspecies p -wave interaction has been discussed in the context of a magnon in a two-dimensional Bose-Bose mixture [72]. Here, we analyze the polaronic neutron excitation by calculating the self-energy for the resonant p -wave neutron-alpha scattering. Furthermore, by considering the residual 1S_0 neutron-neutron attractive interaction, we study the fate of two adjacent polaronic neutrons in dilute alpha matter. The possible occurrence of bound dineutrons due to the polaron effect, which is explored by solving the Bethe-Salpeter equation, may be relevant to the formation of multi-nucleon clusters in neutron-rich nuclei, intermediate energy heavy-ion collisions, and core-collapse supernova cores. Moreover, in the presence of such a bound state, the crossover from dineutron BEC to Bardeen-Cooper-Schrieffer (BCS) neutron superfluid can be anticipated [73]. Also, to understand the physical consequence of the polaron energy in this system, we argue that the polaron energy is associated with the Wigner term in the nuclear energy density [57, 58].

This paper is organized as follows. In Sec. II, the theoretical model and the Bose-polaron formalism will be presented. In Sec. III, we will show the result for the polaronic neutron excitations and therefrom discuss the dineutron formation in the alpha condensate and the implication for the Wigner term. Summary of this paper will be shown in Sec. IV.

II. FORMALISM

Hereinafter, we take $\hbar = k_B = 1$, and the system volume is set to unity.

A. Model

Here, we employ the two-channel Hamiltonian [74] for the $J^\pi = 3/2^-$ ${}^5\text{He}$ resonance, which is relevant at low relative energies, as given by

$$H = H_\nu + H_\alpha + H_\Phi + V_{3/2^-}, \quad (1)$$

where the contribution of spin-1/2 neutrons ($s_z = \pm 1/2$) with a mass M_ν reads

$$H_\nu = \sum_{s_z} \sum_{\mathbf{k}} \xi_{\mathbf{k},\nu} \nu_{\mathbf{k},s_z}^\dagger \nu_{\mathbf{k},s_z}$$

$$+ \sum_{\mathbf{k}, \mathbf{k}', \mathbf{Q}} U_{2\nu}(\mathbf{k}, \mathbf{k}') \nu_{\mathbf{k}+\mathbf{Q}/2, +1/2}^\dagger \nu_{-\mathbf{k}+\mathbf{Q}/2, -1/2}^\dagger \times \nu_{-\mathbf{k}'+\mathbf{Q}/2, -1/2} \nu_{\mathbf{k}'+\mathbf{Q}/2, +1/2} \quad (2)$$

with the neutron kinetic energy $\xi_{\mathbf{k}, \nu} = k^2/2M_\nu$, the neutron creation (annihilation) operator $\nu_{\mathbf{k}, s_z}^{(\dagger)}$, and 1S_0 neutron-neutron coupling $U_{2\nu}(\mathbf{k}, \mathbf{k}')$. The contribution of alpha particles reads

$$H_\alpha = \sum_{\mathbf{q}} \xi_{\mathbf{q}, \alpha} \alpha_{\mathbf{q}}^\dagger \alpha_{\mathbf{q}} + \frac{1}{2} \sum_{\mathbf{q}, \mathbf{q}', \mathbf{K}} U_{2\alpha}(\mathbf{q}, \mathbf{q}') \alpha_{\mathbf{q}+\mathbf{K}/2}^\dagger \alpha_{-\mathbf{q}+\mathbf{K}/2}^\dagger \times \alpha_{-\mathbf{q}'+\mathbf{K}/2} \alpha_{\mathbf{q}'+\mathbf{K}/2} \quad (3)$$

with the alpha-particle kinetic energy $\xi_{\mathbf{q}, \alpha} = q^2/2M_\alpha - \mu_\alpha$ ($M_\alpha = 4M_\nu$ and μ_α are the alpha particle mass and

chemical potential, respectively), the alpha-particle annihilation (creation) operator $\alpha_{\mathbf{q}}^{(\dagger)}$, and the alpha-alpha interaction $U_{2\alpha}(\mathbf{q}, \mathbf{q}')$, and the kinetic term of the closed-channel ^5He state with $J^\pi = 3/2^-$ ($J_z = \pm 1/2, \pm 3/2$) reads

$$H_\Phi = \sum_{\mathbf{P}, J_z} (\xi_{\mathbf{P}, \Phi} + E_\Phi) \Phi_{\mathbf{P}, J_z}^\dagger \Phi_{\mathbf{P}, J_z} \quad (4)$$

with the bare ^5He kinetic energy $\xi_{\mathbf{P}, \Phi} = P^2/2M_r - \mu_\alpha$, the bare ^5He energy level E_Φ [$M_r = (1/M_\nu + 1/M_\alpha)^{-1}$ is the reduced mass], the bare ^5He annihilation (creation) operator $\Phi_{\mathbf{P}, J_z}^{(\dagger)}$. Note that we set the neutron chemical potential to zero since neutrons are regarded as impurities.

The interaction term $V_{3/2^-}$ responsible for the $J^\pi = 3/2^-$ p -wave resonance is given by

$$V_{3/2^-} = \sum_{J_z, s_z, m} \sum_{\mathbf{P}, \mathbf{k}} \left(kg_k \sqrt{\frac{4\pi}{3}} Y_m^{\ell=1}(\hat{\mathbf{k}}) \langle 1, m; 1/2, s_z | 3/2, J_z \rangle \Phi_{\mathbf{P}, J_z}^\dagger \nu_{\mathbf{k}+\mathbf{P}/2, s_z} \alpha_{-\mathbf{k}+\mathbf{P}/2} + \text{h.c.} \right), \quad (5)$$

where $\langle 1, m; 1/2, s_z | 3/2, J_z \rangle$ is the Clebsch-Gordan coefficient. We employ the Yamaguchi-type form factor

$$g_k = \frac{g}{1 + (k/\Lambda)^2}, \quad (6)$$

where Λ is the cutoff scale and g is the coupling strength at $k = 0$. These parameters are related to the low-energy constants as [74]

$$a_p = -\frac{M_r g^2}{6\pi} \left(E_\Phi - \frac{M_r g^2 \Lambda^3}{12\pi} \right)^{-1}, \quad r_p = -\frac{6\pi}{M_r^2 g^2} + \frac{24\pi E_\Phi}{M_r g^2 \Lambda^2} - 3\Lambda. \quad (7)$$

Here, $a_p = -67.1 \text{ fm}^3$ and $r_p = -0.87 \text{ fm}^{-1}$ are the $J^\pi = 3/2^-$ p -wave scattering volume and effective range, respectively [39]. Also, we set $\Lambda = 0.90 \text{ fm}^{-1}$ in such a way as to reproduce the ^5He resonance energy $E_{\text{res}} \sim 0.93 \text{ MeV}$. We can then determine $E_\Phi = 449.607 \text{ MeV}$ and $M_r g^2 = 113.388 \text{ fm}^2$ from the empirical values of a_p and r_p .

B. Bose-polaron self-energy

As for a medium of dilute symmetric nuclear matter, we consider a zero-temperature alpha condensate. The alpha condensate density denoted by ρ_α controls the polaronic properties of an impurity neutron. Within the mean-field approximation, the alpha condensation energy

density reads $\mathcal{E}_\alpha = -\mu_\alpha \rho_\alpha + \frac{1}{2} U_{2\alpha}(\mathbf{0}, \mathbf{0}) \rho_\alpha^2$, from which

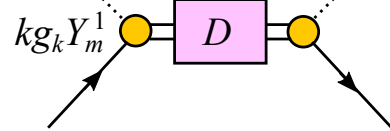


FIG. 2. Beliaev-type self-energy of a polaronic neutron in an alpha condensate, which is accompanied by the dressed ^5He propagator D . The dotted line describes the alpha condensate wave function or, equivalently, the square root of the condensate density $\sqrt{\rho_\alpha}$. The circles represent the neutron-alpha- ^5He coupling $kg_k Y_m^1$ within the $J^\pi = 3/2^-$ channel.

we obtain $\mu_\alpha = U_{2\alpha}(\mathbf{0}, \mathbf{0}) \rho_\alpha$. However, since the value of $U_{2\alpha}(\mathbf{0}, \mathbf{0})$ has a large uncertainty in the matter, for simplicity, we take $\mu_\alpha \simeq 0$, which is valid in the dilute regime. In this regard, the information on the alpha condensate is incorporated only via ρ_α .

We are interested in the neutron retarded Green's function

$$G_{s_z}(\mathbf{k}, \omega) = \frac{1}{\omega_+ - \xi_{\mathbf{k}, \nu} - \Sigma_{s_z}(\mathbf{k}, \omega)}, \quad (8)$$

where $\omega_+ = \omega + i\delta$ involves an infinitesimally small imaginary number $i\delta$. Then, the self-energy of a neutron embedded in the alpha condensate is given by the Beliaev-type diagram [47]:

$$\Sigma_{s_z}(\mathbf{k}, \omega) = \frac{4\pi}{3} k^2 \rho_\alpha \sum_{J_z} \sum_m \langle 1, m; 1/2, s_z | 3/2, J_z \rangle^2 g_k^2 Y_m^1(\hat{\mathbf{k}}) [Y_m^1(\hat{\mathbf{k}})]^* D_{J_z}(\mathbf{k}, \omega), \quad (9)$$

which incorporates the resonant scattering between a neutron with momentum \mathbf{k} and an alpha particle at zero momentum. (i.e., in the condensate). More explicitly, in the case of $s_z = +1/2$, we obtain

$$\Sigma_{1/2}(\mathbf{k}, \omega) = g_k^2 \rho_\alpha \left[\frac{k_x^2 + k_y^2}{2} D_{3/2}(\mathbf{k}, \omega) + \frac{k_x^2 + k_y^2 + 4k_z^2}{6} D_{1/2}(\mathbf{k}, \omega) \right], \quad (10)$$

where the dressed ^5He propagators $D_{J_z}(\mathbf{k}, \omega)$ are given by

$$D_{J_z}(\mathbf{k}, \omega) = \frac{1}{\omega_+ - \xi_{\mathbf{k}, \Phi} - E_\Phi - \Pi_{J_z}(\mathbf{k}, \omega)}. \quad (11)$$

Note that $\Sigma_{s_z=-1/2}(\mathbf{k}, \omega) = \Sigma_{s_z=1/2}(\mathbf{k}, \omega)$. The one-loop self-energy $\Pi_{J_z}(\mathbf{k}, \omega)$ for the neutron-alpha scattering reads

$$\Pi_{3/2}(\mathbf{P}, \Omega) = \sum_{\mathbf{q}} g_q^2 \left(\frac{q_x^2 + q_y^2}{2} \right) \times \frac{1}{\Omega_+ - \xi_{\mathbf{q}+\mathbf{P}/2, \nu} - \xi_{-\mathbf{q}+\mathbf{P}/2, \alpha}}, \quad (12)$$

$$\Pi_{1/2}(\mathbf{P}, \Omega) = \sum_{\mathbf{q}} g_q^2 \left(\frac{2}{3} q_z^2 + \frac{q_x^2 + q_y^2}{6} \right) \times \frac{1}{\Omega_+ - \xi_{\mathbf{q}+\mathbf{P}/2, \nu} - \xi_{-\mathbf{q}+\mathbf{P}/2, \alpha}}. \quad (13)$$

III. RESULTS

Let us now exhibit numerical results for the properties of a Bose-polaronic neutron and the resultant implications for the bound dineutron and the Wigner energy.

A. Polaronic neutron in the alpha condensate

Since we are interested in the low-energy quasiparticle properties of a neutron immersed in the alpha condensate, we perform the low-momentum expansion of $\Sigma_{s_z}(\mathbf{k}, \omega)$. First, one can find

$$\Sigma_{s_z}(\mathbf{k} = 0, \omega) = 0, \quad (14)$$

because $\Sigma_{s_z}(\mathbf{k}, \omega)$ is always proportional to k^2 due to the p -wave properties. Accordingly, the p -wave polaron energy E_P is zero (i.e., $E_P = \Sigma_{s_z}(\mathbf{k} = 0, \omega) = 0$). We

expand $\Sigma_{s_z}(\mathbf{k}, \omega)$ around $\mathbf{k} = 0$ and $\omega = \xi_{\mathbf{k}=0, \nu} = 0$ as

$$\begin{aligned} \Sigma_{s_z}(\mathbf{k}, \omega) &\simeq \Sigma_{s_z}(\mathbf{0}, \xi_{\mathbf{0}, \nu}) \\ &+ \left. \frac{\partial \Sigma_{s_z}(\mathbf{0}, \omega)}{\partial \omega} \right|_{\omega=\xi_{\mathbf{0}, \nu}} (\omega - \xi_{\mathbf{0}, \nu}) \\ &+ \frac{1}{2} \sum_{j=x,y,z} \left. \frac{\partial^2 \Sigma_{s_z}(\mathbf{k}, \xi_{\mathbf{0}, \nu})}{\partial k_j^2} \right|_{k_j=0} k_j^2. \end{aligned} \quad (15)$$

In this way, we obtain the approximate form of polaronic neutron Green's function

$$\begin{aligned} G_{s_z}(\mathbf{k}, \omega) &= \frac{1}{\omega_+ - \xi_{\mathbf{k}, \nu} - \Sigma_{s_z}(\mathbf{k}, \omega)} \\ &\simeq \frac{Z}{\omega_+ - \sum_j \frac{k_j^2}{2M_{\text{eff}, j}} + i\Gamma_P/2}, \end{aligned} \quad (16)$$

where $\Sigma_{s_z}(\mathbf{0}, \xi_{\mathbf{0}, \nu}) = 0$. In the present case, the effective mass $M_{\text{eff}, j=x,y,z}$ is not necessarily isotropic as in the case of polarons in dipolar Fermi gases [75]. Here, we define the quasiparticle residue

$$Z = \left[1 - \text{Re} \left. \frac{\partial \Sigma_{s_z}(\mathbf{k}, \omega)}{\partial \omega} \right|_{\omega=0} \right]^{-1}, \quad (17)$$

and the inverse effective mass

$$\frac{M_\nu}{M_{\text{eff}, j}} = Z \left[1 + M \text{Re} \left. \frac{\partial^2 \Sigma_{s_z}(\mathbf{0}, \xi_{\mathbf{0}, \nu})}{\partial k_j^2} \right|_{k_j=0} \right]. \quad (18)$$

The low-momentum expansion of $\Sigma_{s_z}(\mathbf{k}, \omega)$ reads

$$\Sigma_{s_z}(\mathbf{k}, \omega) = \frac{2}{3} \frac{g^2 \rho_\alpha k^2}{\omega_+ - E_\Phi - \Pi_0(\omega)} + O(k^4), \quad (19)$$

where we used

$$\begin{aligned} D_{J_z}(\mathbf{k}, \omega) &= D_{J_z}(\mathbf{0}, \omega) + O(k^2) \\ &\equiv \frac{1}{\omega_+ - E_\Phi - \Pi_0(\omega)} + O(k^2) \end{aligned} \quad (20)$$

with $\Pi_0(\omega) \equiv \Pi_{3/2}(\mathbf{0}, \omega) = \Pi_{1/2}(\mathbf{0}, \omega)$ given by

$$\Pi_0(\omega) = -\frac{M_r g^2 \Lambda^4 [\Lambda^3 + 6\Lambda M_r \omega + 2i(2M_r \omega)^{3/2}]}{12\pi(2M_r \omega + \Lambda^2)^2}. \quad (21)$$

In particular, we obtain

$$\Pi_0(0) = -\frac{M_r g^2 \Lambda^3}{12\pi}. \quad (22)$$

This result indicates that the neutron effective mass is isotropic ($M_{\text{eff}, x} = M_{\text{eff}, y} = M_{\text{eff}, z} \equiv M_{\text{eff}}$) in the low-momentum limit. Indeed, we analytically obtain

$$\left. \frac{\partial^2 \Sigma_{s_z}(\mathbf{k}, 0)}{\partial k^2} \right|_{\mathbf{k}=0} = -\frac{8\pi a_p}{M_r} \rho_\alpha. \quad (23)$$

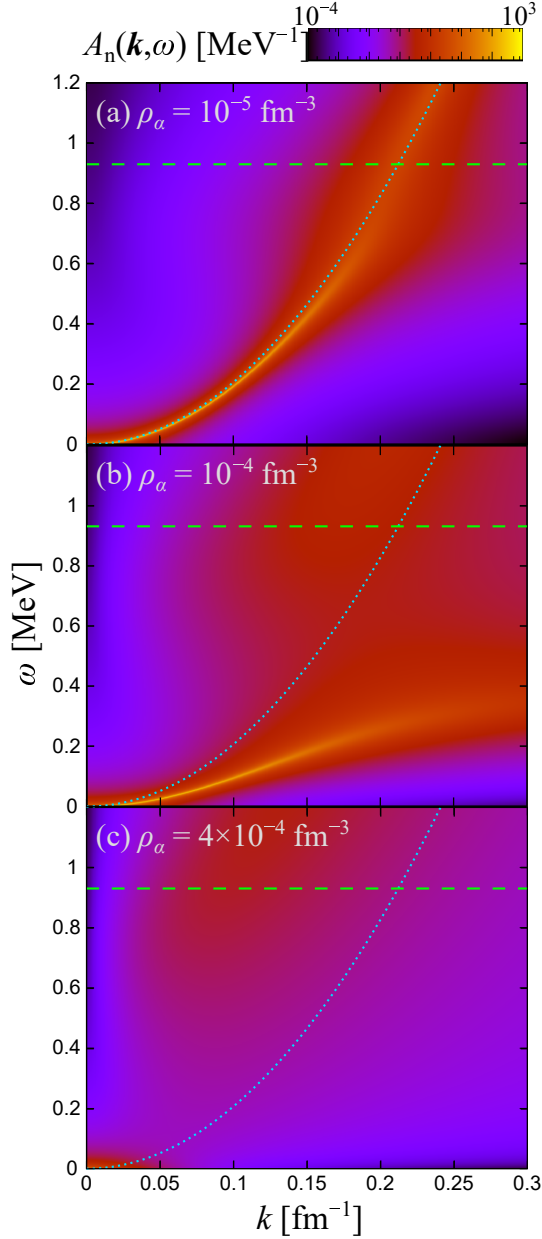


FIG. 3. Low-momentum neutron-polaron spectral weight $A_n(\mathbf{k}, \omega)$ in the alpha condensate. For comparison, the bare neutron dispersion $\xi_{\mathbf{k}, \nu} = k^2/2M_\nu$ (dotted curve) is plotted in each panel. The dashed line shows the empirical resonance position of ${}^5\text{He}$ at rest. The alpha condensation densities are taken as (a) $\rho_\alpha = 10^{-5} \text{ fm}^{-3}$, (b) $\rho_\alpha = 10^{-4} \text{ fm}^{-3}$, and (c) $\rho_\alpha = 4 \times 10^{-4} \text{ fm}^{-3}$. Strictly speaking, at nonzero k , the resonance position is shifted by the amount of the center-of-mass ${}^5\text{He}$ kinetic energy $(M_\nu k)^2/2(M_\nu + M_\alpha)^3$, which is negligible compared with $\xi_{\mathbf{k}, \nu}$.

Moreover, one can find

$$\frac{\partial \Sigma_{s_z}(\mathbf{0}, \omega)}{\partial \omega} = 0, \rightarrow Z = 1, \quad (24)$$

$$\text{Im} \Sigma_{s_z}(\mathbf{0}, \omega) = 0, \rightarrow \Gamma_P = 0. \quad (25)$$

Since $Z \rightarrow 1$ in (18), we obtain

$$\frac{M_\nu}{M_{\text{eff}}} = 1 + \frac{8\pi M_\nu a_p \rho_\alpha}{M_r} < 1 \quad (a_p < 0), \quad (26)$$

indicating the heavier effective mass compared to the bare one. Eventually, formation of a bound dineutron in the alpha condensate is possible with the help of the induced interaction [76].

If the alpha-condensation density increases further, the effective mass diverges at

$$\rho_c = \frac{1}{8\pi|a_p|} \frac{M_\alpha}{M_\nu + M_\alpha} \simeq 4.74 \times 10^{-4} \text{ fm}^{-3}. \quad (27)$$

Beyond ρ_c , the effective mass of a polaronic neutron becomes negative, indicating a breakdown of the low-momentum polaron picture in the rest frame of the homogeneous alpha condensate and possibly a signature of self-localization of a polaronic neutron as discussed in Refs. [72, 77, 78]. This is in sharp contrast with p -wave Fermi polarons [70, 71], of which a transition to a Feshbach molecular state was predicted to occur. We also note that the negative effective mass was discussed in repulsive Fermi polarons as a precursor of ferromagnetic instability [79]. Although we do not consider the alpha-alpha interaction and resulting quantum depletion explicitly, such effects would not change the result for the effective mass drastically. In fact, it is reported that the effective mass is not strongly affected by the boson-boson interaction in the case of s -wave Bose polarons [47].

Strictly speaking, however, the alpha-alpha interaction should affect various properties of the medium itself even at $\rho \approx \rho_c$. For example, $4\rho_c$ are not necessarily equal to the critical value of the total nucleon density because the depletion of the condensate due to quantum fluctuations occurs even at $T = 0$. Indeed, such a depletion is predicted to originate from the inter-alpha interactions and the in-medium breakup of alpha particles themselves [80]. Therefore, ρ_c may well be regarded as the critical density for the condensate component of alpha matter (not for the whole system). Then, the corresponding total nucleon density could be much higher than $4\rho_c$, which suggests that the system is more like a liquid state rather than a gas state as usually assumed in earlier investigations [81].

Figure 3 shows the polaronic neutron spectral weight

$$A_n(\mathbf{k}, \omega) = -\frac{1}{\pi} \text{Im} G_{s_z}(\mathbf{k}, \omega), \quad (28)$$

where we used the low-momentum expression for the self-energy given by Eq. (19) and omitted the spin index. For the overall structure, one can see that a sharp peak remains typically up to the threshold momentum of ${}^5\text{He}$ given by $\sqrt{2M_\nu E_{\text{res}}} \simeq 0.21 \text{ fm}^{-1}$ in the low-density regime. This is due to the level repulsion between the polaronic neutron branch and the ${}^5\text{He}$ molecular branch. In the low-density regime (e.g., at $\rho_\alpha = 10^{-5} \text{ fm}^{-3}$ in Fig. 3), one can see that the quasiparticle peak is located

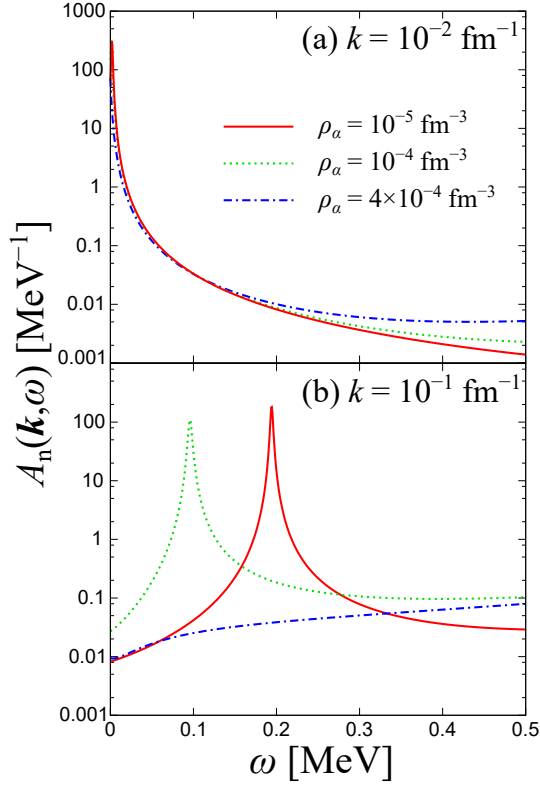


FIG. 4. Polaronic neutron spectral weight $A_n(\mathbf{k}, \omega)$ with fixed momenta [(a) $k = 10^{-2} \text{ fm}^{-1}$ and (b) $k = 10^{-1} \text{ fm}^{-1}$] in the alpha condensate.

close to the bare dispersion $\xi_{\mathbf{k}, \nu} = k^2/2M_\nu$ and that the spectral broadening occurs near the ${}^5\text{He}$ resonance. At $\rho_\alpha = 10^{-4} \text{ fm}^{-3}$, as shown in Fig. 3, there is a deviation between the spectral peak and the bare dispersion in such a way that the effective mass of the polaronic neutron branch becomes larger than the bare one. Moreover, the spectral broadening due to the coupling with the ${}^5\text{He}$ branch is more prominent than the low-density result. Finally, just below $\rho_\alpha = \rho_c = 4.74 \times 10^{-4} \text{ fm}^{-3}$, as shown in Fig. 3 where we set $\rho_\alpha = 4 \times 10^{-4} \text{ fm}^{-3}$, the spectral weight is flattened in the low-momentum limit, which corresponds to the almost divergent effective mass, while the spectral broadening increases with neutron momentum.

To see more detailed structure of the neutron spectral weight, we plot $A_n(\mathbf{k}, \omega)$ at fixed momenta and different ρ_α in Fig. 4, where $k = 10^{-2} \text{ fm}^{-1}$ and $k = 10^{-1} \text{ fm}^{-1}$ are taken in the panels (a) and (b), respectively. At a sufficiently small momentum as shown in the panel (a) of Fig. 4, a stable polaron peak can be found even near the critical density. Building the high-frequency limit of

Eq. (21),

$$\Pi_0(\omega \rightarrow \infty) \rightarrow -i \frac{M_r g^2 \Lambda^4}{6\pi \sqrt{2M_r} \omega}, \quad (29)$$

into $\text{Im}\Sigma_{s_z}(\mathbf{k}, \omega \rightarrow \infty)$ as

$$\begin{aligned} \text{Im}\Sigma_{s_z}(\mathbf{k}, \omega \rightarrow \infty) &\rightarrow \frac{2}{3} \frac{g^2 \rho_\alpha k^2 \text{Im}\Pi_0(\omega \rightarrow \infty)}{\omega^2} + O(k^4) \\ &\equiv -\frac{M_r g^4 \Lambda^4 \rho_\alpha k^2}{9\pi \sqrt{2M_r} \omega^{5/2}} + O(k^4), \end{aligned} \quad (30)$$

we obtain the high-frequency tail of the spectral weight as

$$A_n(\mathbf{k}, \omega) \rightarrow \frac{M_r g^4 \Lambda^4 \rho_\alpha k^2}{9\pi^2 \sqrt{2M_r} \omega^{9/2}} + O(k^4), \quad (31)$$

indicating that the high-frequency tail is proportional to ρ_α as well as k^2 . Indeed, Fig. 4(a) shows the enhancement of the high-frequency spectra with increasing ρ_α . As shown in Fig. 4(b), at a larger momentum, the polaron peak is shifted towards high frequencies in such a way as to follow the dispersion relation $k^2/2M_{\text{eff}}$ at relatively small ρ_α . However, the polaron peak at this momentum is no longer visible at $\rho_\alpha = 4 \times 10^{-4} \text{ fm}^{-3}$ being close to ρ_c . We remark in passing that in a manner that is consistent with the k dependence of Eq. (31), the high-frequency contribution in the panel (b) is significantly larger than that in the panel (a).

B. Dineutrons in the alpha condensate

Here, we show that a dineutron can be a bound state due to the enhanced M_{eff} together with the 1S_0 neutron-neutron interaction $U(k, k')$. A similar binding mechanism of two alpha particles in dilute neutron matter has been examined theoretically [40]. On the basis of the results of polaronic neutron spectra shown in Fig. 3, we employ the approximate form of the thermal neutron propagator in dilute alpha matter as

$$\tilde{G}_{s_z}(\mathbf{k}, i\omega_n) = \frac{\theta(k_c - k)}{i\omega_n - \frac{k^2}{2M_{\text{eff}}}} + \frac{\theta(k - k_c)}{i\omega_n - \frac{k^2}{2M_\nu}}, \quad (32)$$

with the fermion Matsubara frequency $\omega_n = (2n + 1)\pi T$ ($n \in \mathbb{Z}$), where we have assumed that the low-energy polaron state is valid up to some momentum cutoff k_c . The precise value of k_c , which is controlled by the properties of the alpha condensate and the neutron-alpha interaction, remains to be known and hence will be taken arbitrarily in the range of $0.1 \text{ fm}^{-1} \lesssim k_c \lesssim 10 \text{ fm}^{-1}$. Above $k = k_c$, we consider two bare neutrons in a virtual state. For simplicity, the effects of the spectral broadening near the ${}^5\text{He}$ resonance are neglected. The two-neutron T -matrix $T_{2\nu}(k, k', i\Omega_\ell)$ with the boson Matsubara frequency $\Omega_\ell = 2\ell\pi T$ ($\ell \in \mathbb{Z}$) in the 1S_0 channel is given by

$$T_{2\nu}(k, k', i\Omega_\ell) = U_{2\nu}(k, k') - T \sum_{\mathbf{q}, i\omega_n} U_{2\nu}(k, q) \tilde{G}_{+1/2}(\mathbf{q}, i\omega_n + i\Omega_\ell) \tilde{G}_{-1/2}(-\mathbf{q}, -i\omega_n) T_{2\nu}(q, k, i\Omega_\ell). \quad (33)$$

Using the separable 1S_0 neutron-neutron interaction $U_{2\nu}(k, k') = U_0 \chi_k \chi_{k'}$ with the form factor χ_k to be specified below, we obtain $T_{2\nu}(k, k'; i\Omega_\ell) = t_{2\nu}(i\Omega_\ell) \chi_k \chi_{k'}$ with

$$t_{2\nu}(i\Omega_\ell) = \frac{U_0}{1 - U_0 \Xi(i\Omega_\ell)}, \quad (34)$$

where the polarization function Ξ reads

$$\begin{aligned} \Xi(i\Omega_\ell) &= -T \sum_{\mathbf{q}, i\omega_n} \chi_q^2 \tilde{G}_{+1/2}(\mathbf{q}, i\omega_n + i\Omega_\ell) \tilde{G}_{-1/2}(-\mathbf{q}, -i\omega_n) \\ &= \sum_{\mathbf{q}} \frac{\chi_q^2 \theta(k_c - q)}{i\Omega_\ell - q^2/M_{\text{eff}}} + \sum_{\mathbf{q}} \frac{\chi_q^2 \theta(q - k_c)}{i\Omega_\ell - q^2/M_\nu}. \end{aligned} \quad (35)$$

After the analytical continuation to the real frequency ($i\Omega_\ell \rightarrow \Omega + i\delta$), the dineutron binding energy E_{nn} can be

obtained from

$$1 - U_0 \Xi(\Omega = -E_{\text{nn}}) = 0. \quad (36)$$

Practically, we use

$$\chi_q = \frac{1}{\sqrt{1 + (q/\lambda)^2}}. \quad (37)$$

The parameters U_0 and λ are determined by the 1S_0 scattering length $a_{2\nu} = -18.5$ fm and $r_{2\nu} = 2.8$ fm as [82]

$$U_0 = \frac{4\pi a_{2\nu}}{M_\nu} \frac{1}{1 - a_{2\nu}\lambda}, \quad (38)$$

$$\lambda = \frac{1}{r_{2\nu}} \left(1 + \sqrt{1 - \frac{2r_{2\nu}}{a_{2\nu}}} \right). \quad (39)$$

Moreover, one can perform the momentum summation in Eq. (35) as

$$\begin{aligned} \Xi(-E_{\text{nn}}) &= -\frac{M_\nu \lambda^2}{2\pi^2} \left[\frac{M_{\text{eff}}}{M_\nu} \frac{\lambda \tan^{-1}\left(\frac{k_c}{\lambda}\right) - \sqrt{M_{\text{eff}} E_{\text{nn}}} \tan^{-1}\left(\frac{k_c}{\sqrt{M_{\text{eff}} E_{\text{nn}}}}\right)}{\lambda^2 - M_{\text{eff}} E_{\text{nn}}} \right. \\ &\quad \left. + \frac{\pi}{2} \frac{1}{\lambda + \sqrt{M_\nu E_{\text{nn}}}} - \frac{\lambda \tan^{-1}\left(\frac{k_c}{\lambda}\right) - \sqrt{M_\nu E_{\text{nn}}} \tan^{-1}\left(\frac{k_c}{\sqrt{M_\nu E_{\text{nn}}}}\right)}{\lambda^2 - M_\nu E_{\text{nn}}} \right]. \end{aligned} \quad (40)$$

In this way, the bound-state equation reads

$$\begin{aligned} 1 - \frac{1}{a_{2\nu}\lambda} &= \frac{2}{\pi} \left[\frac{M_{\text{eff}}}{M_\nu} \frac{\tan^{-1}\left(\frac{k_c}{\lambda}\right) - \sqrt{\frac{M_{\text{eff}}}{M_\nu} \frac{M_\nu E_{\text{nn}}}{\lambda^2}} \tan^{-1}\left(\frac{k_c}{\lambda} \sqrt{\frac{M_\nu}{M_{\text{eff}}}} \frac{\lambda^2}{M_\nu E_{\text{nn}}}\right)}{1 - \frac{M_{\text{eff}}}{M_\nu} \frac{M_\nu E_{\text{nn}}}{\lambda^2}} \right. \\ &\quad \left. + \frac{\pi}{2} \frac{1}{1 + \sqrt{\frac{M_\nu E_{\text{nn}}}{\lambda^2}}} - \frac{\tan^{-1}\left(\frac{k_c}{\lambda}\right) - \sqrt{\frac{M_\nu E_{\text{nn}}}{\lambda^2}} \tan^{-1}\left(\frac{k_c}{\lambda} \sqrt{\frac{\lambda^2}{M_\nu E_{\text{nn}}}}\right)}{1 - \frac{M_\nu E_{\text{nn}}}{\lambda^2}} \right]. \end{aligned} \quad (41)$$

The numerical results for E_{nn} that can be obtained from Eq. (41) are shown in Fig. 5. These results indicate that dineutrons can be bound due only to the effective-mass acquisition of polaronic neutrons and the direct 1S_0 neutron-neutron interaction, even without the help of the medium-induced interaction. In this case, there is a threshold effective mass $M_{\text{eff},c}$ for the presence of a bound dineutron, which can be obtained by taking $E_{\text{nn}} = 0$ in

Eq. (41) as

$$\frac{M_{\text{eff},c}}{M_\nu} = 1 - \frac{\pi}{2a_{2\nu}\lambda \tan^{-1}\left(\frac{k_c}{\lambda}\right)}. \quad (42)$$

Here, one needs to examine the cutoff-parameter dependence of E_{nn} and $M_{\text{eff},c}$. As shown in Fig. 5 where several different values of k_c/λ are taken with λ fixed at 0.765 fm^{-1} [see Eq. (39)], E_{nn} increases with k_c . This is because for larger k_c , each neutron more often behaves like a polaronic massive particle; according to Eq. (41),

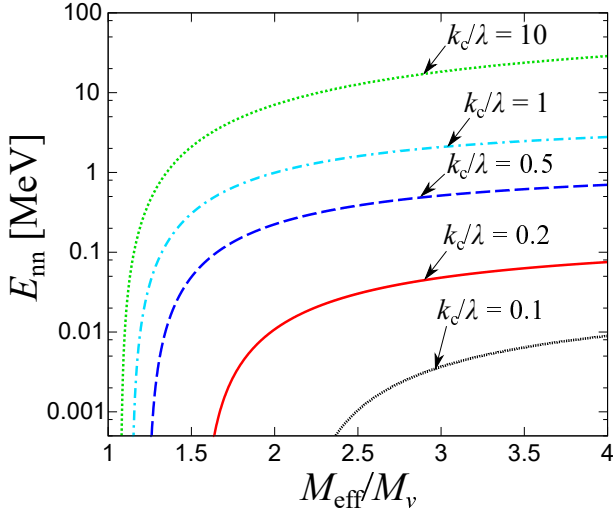


FIG. 5. Dineutron binding energy E_{nn} in dilute alpha matter as a function of the effective mass M_{eff} of a polaronic neutron with various values of the cutoff parameter k_c divided by $\lambda = 0.765 \text{ fm}^{-1}$.

for $k_c \gg \lambda$ where $\tan^{-1}(k_c/\lambda) \simeq \pi/2$, E_{nn} is close to its upper limit $\lambda^2/M_{\text{eff}}[(M_{\text{eff}}/M_\nu)/(1 - 1/a_{2\nu}\lambda) - 1]^2$, while for $k_c \ll \lambda$ where $\tan^{-1}(k_c/\lambda) \simeq k_c/\lambda$, the condition for $E_{nn} > 0$ is sensitive to the value of k_c . Also, $M_{\text{eff},c}$ tends to decrease with increasing k_c , as is clear from Eq. (42). While the notable k_c dependence of E_{nn} can be found in Fig. 5, it would be fair to employ $k_c/\lambda = 0.2$ (i.e., $k_c \simeq 0.15 \text{ fm}^{-1}$), below which the polaronic spectral weight exhibits a sharp quasiparticle peak as shown in Figs. 3(a) and (b).

Finally, in Fig. 6, we show the effective mass M_{eff} of a polaronic neutron as a function of ρ_α . For comparison, we also show the critical effective mass $M_{\text{eff},c}$ for the formation of a bound dineutron in the case of $k_c/\lambda = 0.2$. In this case, a bound dineutron starts to appear around $\rho_\alpha \simeq 2 \times 10^{-4} \text{ fm}^{-3}$, where polaronic neutrons remain stable and become sufficiently massive. Such kind of formation of bound dineutrons might be relevant to the alpha and dineutron clustering structure of neutron-rich light nuclei such as ^8He [33] and ^{10}Be [83, 84]. While the condensation density ρ_α is substantially lower than normal nuclear density, as already discussed in the previous subsection, ρ_α could be substantially lower than the total alpha density including the effects of quantum depletion. Also, the dineutron formation in the alpha condensate via the neutron-alpha p -wave coupling is similar to the structure of two-neutron halo nuclei such as ^6He and ^{11}Li . To take a closer look at this similarity, the $J^\pi = 1/2^-$ channel as neglected in the present study would have to be taken into account.

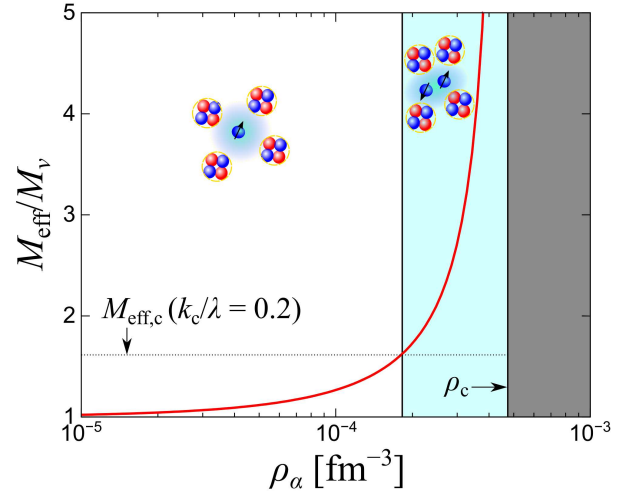


FIG. 6. Effective mass M_{eff} of a polaronic neutron plotted as a function of the alpha condensation density ρ_α . The horizontal dotted line shows the critical effective mass $M_{\text{eff},c}$ for the presence of a bound dineutron in the case of $k_c/\lambda = 0.2$; for momenta below this k_c , a sharp peak can be seen in the calculated neutron spectral weight. ρ_c is the critical alpha condensation density given by Eq. (27). In the shaded region beyond $\rho = \rho_c$, the polaronic neutron experiences divergence of the effective mass, indicating the breakdown of the low-momentum polaron picture and possibly the resultant self-localization [72, 77, 78].

C. Wigner term

Finally, we discuss how the energy of a polaronic neutron is related to the Wigner term. The origin of the Wigner term has been considered for decades: Wigner's supermultiplet $SU(4)$ symmetry and/or the isoscalar neutron-proton pairing may cause the Wigner term, while the contribution of each possible origin to the Wigner energy relative to the symmetry energy is different from each other [85–93].

At $T = 0$, the energy per nucleon \mathcal{E}/ρ_A of the system with neutron density ρ_ν ($\ll \rho_A \equiv 4\rho_\alpha^{\text{tot}}$ where ρ_A is the nucleon density in a nucleus with a mass number A and ρ_α^{tot} is the total alpha density) can be written in the form

$$\frac{\mathcal{E}}{\rho_A^{\text{tot}}} = \frac{\mathcal{E}_{\text{SNM}}}{\rho_A^{\text{tot}}} + \frac{E_P}{4} \left(\frac{\rho_\nu}{\rho_\alpha^{\text{tot}}} \right) + O((\rho_\nu/\rho_\alpha^{\text{tot}})^2), \quad (43)$$

where we have assumed that the internal energy density of symmetric nuclear matter \mathcal{E}_{SNM} is equal to \mathcal{E}_α in the low-density limit for simplicity. Then, in \mathcal{E}_{SNM} , the depletion of the alpha condensate can be ignored, but we shall consider the presence of a non-condensed fraction of alpha particles just to ensure the empirical nucleon density in symmetric and nearly symmetric nuclei. For a small isospin asymmetry, E_P may well control the Wigner energy term $E_W \propto |N - Z|$ (i.e., $E_W \propto \rho_\nu$ up to leading order with respect to the isospin asymmetry) in the nuclear energy density [86]. Recall that $E_P = 0$ in the

present p -wave case and that the neutron-alpha s -wave interaction, which is repulsive, has been ignored so far. Such repulsion could become a source of the Wigner term. Indeed, with the s -wave neutron-alpha scattering length $a_s = 2.64$ fm [39], we find the Hartree contribution

$$E_P = \frac{2\pi a_s}{M_r} \rho_\alpha, \quad (44)$$

leading to the Wigner energy of a nucleus given by

$$E_W \equiv \frac{AE_P}{4} \left(\frac{\rho_\nu}{\rho_\alpha^{\text{tot}}} \right) \simeq \frac{\pi a_s}{2M_r} AC \rho_0 \frac{|N - Z|}{A}, \quad (45)$$

where we have approximated ρ_ν as $\rho_0 |N - Z|/A$ ($\rho_0 = 0.16$ fm $^{-3}$ is the normal nuclear density) and introduced the alpha condensate fraction $\mathcal{C} = \rho_\alpha/\rho_\alpha^{\text{tot}}$.

Let us now make a comparison with the empirical Wigner term, which is included in the nuclear mass formulas. To this end, it is important to evaluate Eq. (45). For typical \mathcal{C} , we consider a small value $\mathcal{C} \simeq 4\rho_c/\rho_0 \simeq 0.012$ since our approach is valid up to $\rho_\alpha = \rho_c$. For reference, in ^4He superfluid droplets, the condensate fraction \mathcal{C} is less than 0.1 even around zero temperature [94]. Then, possible alpha condensed nuclei may involve stronger quantum fluctuations than the ^4He counterpart, leading to the smaller condensate fraction [95]. In this way, we obtain $E_W \simeq 0.41 |N - Z|$ MeV. This prediction can be compared with the Wigner term in the empirical Koura-Tachibara-Ueno-Yamada (KTUY) mass formula [62, 96], which is given by

$$E_W^{\text{KTUY}} = V_W^{\text{KTUY}} \frac{|N - Z|}{A + \alpha_b}, \quad (46)$$

where $\alpha_b = 5$ is a dimensionless parameter and $V_W^{\text{KTUY}} = 38.0024$ MeV. For medium heavy nuclei ($A \approx 100$), the Wigner term is comparable between our prediction and the KTUY parametrization, although the mass-number dependence is different.

It is noteworthy that our approach based on the assumption that symmetric nuclear matter behaves like dilute alpha matter is suitable for even-even nuclei. For odd-odd nuclei, the neutron-proton pairing might play an additional role in the Wigner energy. We also note that a Wigner-energy-like term associated with the cluster formation occurs even in the variational study of bulk asymmetric nuclear matter [97]. We thus expect that clustering and impurity physics eventually become the key to understanding the Wigner energy.

IV. SUMMARY

In this paper, we have investigated the properties of a polaronic neutron in dilute alpha matter; the Bose polaron picture adopted here has been extensively examined in cold-atomic physics. We have shown that each polaronic neutron undergoes a large enhancement of the effective mass, a vanishing decay, and a constant quasiparticle residue, because of the resonant p -wave coupling with the alpha condensate. Such effective mass enhancement helps to form bound dineutrons, together with the 1S_0 neutron-neutron attraction, which is not sufficiently strong to induce the dineutron binding in a vacuum. Moreover, we clarify how the polaron energy, which occurs due to the s -wave neutron-alpha repulsion, is related to the Wigner term.

To examine more quantitative properties of polaronic neutrons and dineutrons, effects of the anisotropic dispersion and nonzero decay width of polarons, finite temperature, the alpha-mediated interaction between polarons, and larger multi-nucleon clusters will have to be considered. In particular, while we have addressed bound dineutrons only via the increased effective mass and the residual 1S_0 neutron-neutron interaction, the alpha-mediated interaction would further induce a larger dineutron binding energy as in the case of bipolarons [76, 98–102].

For future work associated with the Wigner term, the comparison between the Wigner term and the symmetry energy term both in terms of the polaron energy would be important. The extension to the quartet condensation or quartet BCS models [103–108] for $N = Z$ nuclei would also be a fascinating direction. Moreover, multi-nucleon clusters [14–16] may contribute to the Wigner term at larger $|N - Z|$ as additional corrections (e.g., trineutron and tetra-neutron correlations at $|N - Z| = 3$ and $|N - Z| = 4$, respectively), leading to the non-linearity of \mathcal{E}_W with respect to $|N - Z|$.

ACKNOWLEDGMENTS

H. T. is grateful to S. Furusawa for useful discussion on supernova matter. This work is supported by Grants-in-Aid for Scientific Research provided by JSPS through Nos. JP18H05406, JP22H01158, JP22H01214, JP22K13981, JP22K20372, JP22K25864, JP23H01845, JP23H04526, JP23H01845, JP23K01845, JP23K03426, JP23K22485, JP23K25864, JP24K17057, and JP24K06925. T. N. acknowledges the RIKEN Special Postdoctoral Researcher Program.

-
- [1] J. Blaizot, Nuclear compressibilities, *Phys. Rep.* **64**, 171 (1980).
 [2] H. Heiselberg, C. J. Pethick, and D. G. Ravenhall, Insta-

- bilities in hot nuclear matter: A mechanism for nuclear fragmentation, *Phys. Rev. Lett.* **61**, 818 (1988).
 [3] M. Pfützner, M. Karny, L. V. Grigorenko, and K. Ri-

- isager, Radioactive decays at limits of nuclear stability, *Rev. Mod. Phys.* **84**, 567 (2012).
- [4] M. Oertel, M. Hempel, T. Klähn, and S. Typel, Equations of state for supernovae and compact stars, *Rev. Mod. Phys.* **89**, 015007 (2017).
- [5] L. M. Satarov, I. N. Mishustin, A. Motornenko, V. Vovchenko, M. I. Gorenstein, and H. Stoecker, Phase transitions and Bose-Einstein condensation in α -nucleon matter, *Phys. Rev. C* **99**, 024909 (2019).
- [6] L. M. Satarov, M. I. Gorenstein, I. N. Mishustin, and H. Stoecker, Possible Bose-Einstein condensation of α particles in the ground state of nuclear matter, *Phys. Rev. C* **101**, 024913 (2020).
- [7] S. Furusawa and I. Mishustin, Degeneracy effects and Bose condensation in warm nuclear matter with light and heavy clusters, *Nucl. Phys. A* **1002**, 121991 (2020).
- [8] L. M. Satarov, R. V. Poberezhnyuk, I. N. Mishustin, and H. Stoecker, Phase diagram of α matter with a Skyrme-like scalar interaction, *Phys. Rev. C* **103**, 024301 (2021).
- [9] F. Hoyle, Resonances and nuclear molecular configurations in heavy-ion reactions, *Astrophys. J. (Suppl.)* **1**, 12 (1954).
- [10] A. Tohsaki, H. Horiuchi, P. Schuck, and G. Röpke, Alpha Cluster Condensation in ^{12}C and ^{16}O , *Phys. Rev. Lett.* **87**, 192501 (2001).
- [11] Y. Funaki, T. Yamada, H. Horiuchi, G. Röpke, P. Schuck, and A. Tohsaki, α -Particle Condensation in ^{16}O Studied with a Full Four-Body Orthogonality Condition Model Calculation, *Phys. Rev. Lett.* **101**, 082502 (2008).
- [12] T. Wakasa, E. Ihara, K. Fujita, Y. Funaki, K. Hatanaka, H. Horiuchi, M. Itoh, J. Kamiya, G. Röpke, H. Sakaguchi, N. Sakamoto, Y. Sakemi, P. Schuck, Y. Shimizu, M. Takashina, S. Terashima, A. Tohsaki, M. Uchida, H. Yoshida, and M. Yosoi, New candidate for an alpha cluster condensed state in ^{16}O (α, α') at 400 MeV, *Phys. Lett. B* **653**, 173 (2007).
- [13] S. Adachi, Y. Fujikawa, T. Kawabata, H. Akimune, T. Doi, T. Furuno, T. Harada, K. Inaba, S. Ishida, M. Itoh, C. Iwamoto, N. Kobayashi, Y. Maeda, Y. Matsuda, M. Murata, S. Okamoto, A. Sakaue, R. Sekiya, A. Tamii, and M. Tsumura, Candidates for the 5α condensed state in ^{20}Ne , *Phys. Lett. B* **819**, 136411 (2021).
- [14] K. Kisamori, S. Shimoura, H. Miya, S. Michimasa, S. Ota, M. Assie, H. Baba, T. Baba, D. Beaumel, M. Dozono, T. Fujii, N. Fukuda, S. Go, F. Hamache, E. Ideguchi, N. Inabe, M. Itoh, D. Kameda, S. Kawase, T. Kawabata, M. Kobayashi, Y. Kondo, T. Kubo, Y. Kubota, M. Kurata-Nishimura, C. S. Lee, Y. Maeda, H. Matsubara, K. Miki, T. Nishi, S. Noji, S. Sakaguchi, H. Sakai, Y. Sasamoto, M. Sasano, H. Sato, Y. Shimizu, A. Stolz, H. Suzuki, M. Takaki, H. Takeda, S. Takeuchi, A. Tamii, L. Tang, H. Tokieda, M. Tsumura, T. Uesaka, K. Yako, Y. Yanagisawa, R. Yokoyama, and K. Yoshida, Candidate Resonant Tetraneutron State Populated by the $^4\text{He}(^8\text{He}, ^8\text{Be})$ Reaction, *Phys. Rev. Lett.* **116**, 052501 (2016).
- [15] T. Faestermann, A. Bergmaier, R. Gernhäuser, D. Koll, and M. Mahgoub, Indications for a bound tetraneutron, *Phys. Lett. B* **824**, 136799 (2022).
- [16] M. Duer, T. Aumann, R. Gernhäuser, V. Panin, S. Paschalis, D. Rossi, N. Achouri, D. Ahn, H. Baba, C. Bertulani, *et al.*, Observation of a correlated free four-neutron system, *Nature* **606**, 678 (2022).
- [17] K. Miki, K. Kameya, D. Sakai, R. Urayama, N. Imai, S. Ishikawa, S. Michimasa, S. Ota, M. Sasano, H. Takeda, T. Uesaka, H. Haba, M. Hara, Y. Hatano, T. Hayamizu, N. Kobayashi, A. Tamii, S. Adachi, T. Chillery, M. Dozono, Y. Fujikawa, H. Fujita, N. Fukuda, T. Furuno, J. Gao, S. Goto, S. Hanai, S. Hayakawa, Y. Hijikata, K. Himi, Y. Hirai, J. W. Hwang, M. Ichimura, D. Inomoto, M. Inoue, H. Kasahara, T. Kawabata, K. Kishimoto, S. Kitayama, K. Kusaka, J. Li, Y. Maeda, Y. Maruta, T. Matsui, T. Matsuzaki, S. Nakai, H. Nishibata, M. Otake, Y. Saito, H. Sakai, A. Sakaue, H. Sato, K. Sekiguchi, Y. Shimizu, S. Shimoura, L. Stuhl, T. Sumikama, H. Suzuki, R. Tsuji, S. Tsuji, H. Umetsu, Y. Utsuki, T. Wakasa, A. Watanabe, K. Yako, Y. Yanagisawa, N. Yokota, C. Yonemura, K. Yoshida, and M. Yoshimoto (RIBF-SHARAQ11 Collaboration and RCNP-E502 Collaboration), Precise spectroscopy of the $3n$ and $3p$ systems via the $^3\text{H}(t, ^3\text{He})3n$ and $^3\text{He}(^3\text{He}, t)3p$ reactions at intermediate energies, *Phys. Rev. Lett.* **133**, 012501 (2024).
- [18] A. M. Shirokov, G. Papadimitriou, A. I. Mazur, I. A. Mazur, R. Roth, and J. P. Vary, Prediction for a Four-Neutron Resonance, *Phys. Rev. Lett.* **117**, 182502 (2016).
- [19] S. Gandolfi, H.-W. Hammer, P. Klos, J. E. Lynn, and A. Schwenk, Is a Trineutron Resonance Lower in Energy than a Tetraneutron Resonance?, *Phys. Rev. Lett.* **118**, 232501 (2017).
- [20] R. Lazauskas, E. Hiyama, and J. Carbonell, Low Energy Structures in Nuclear Reactions with $4n$ in the Final State, *Phys. Rev. Lett.* **130**, 102501 (2023).
- [21] F. M. Marqués and J. Carbonell, The quest for light multineutron systems, *Eur. Phys. J. A* **57**, 105 (2021).
- [22] H.-W. Hammer, C. Ji, and D. R. Phillips, Effective field theory description of halo nuclei, *J. Phys. G: Nucl. and Part. Phys.* **44**, 103002 (2017).
- [23] I. Tanihata, H. Hamagaki, O. Hashimoto, Y. Shida, N. Yoshikawa, K. Sugimoto, O. Yamakawa, T. Kobayashi, and N. Takahashi, Measurements of Interaction Cross Sections and Nuclear Radii in the Light p -Shell Region, *Phys. Rev. Lett.* **55**, 2676 (1985).
- [24] I. Tanihata, M. Alcorta, D. Bandyopadhyay, R. Bieri, L. Buchmann, B. Davids, N. Galinski, D. Howell, W. Mills, S. Mythili, R. Openshaw, E. Padilla-Rodal, G. Ruprecht, G. Sheffer, A. C. Shotter, M. Trinczek, P. Walden, H. Savajols, T. Roger, M. Caamano, W. Mittig, P. Roussel-Chomaz, R. Kanungo, A. Gallant, M. Notani, G. Savard, and I. J. Thompson, Measurement of the Two-Halo Neutron Transfer Reaction $^1\text{H}(^{11}\text{Li}, ^9\text{Li})^3\text{H}$ at 3A MeV, *Phys. Rev. Lett.* **100**, 192502 (2008).
- [25] M. Labiche, N. A. Orr, F. M. Marqués, J. C. Angélique, L. Axelsson, B. Benoit, U. C. Bergmann, M. J. G. Borge, W. N. Catford, S. P. G. Chappell, N. M. Clarke, G. Costa, N. Curtis, A. D'Arrigo, E. de Góes Brennand, O. Dorvaux, G. Fazio, M. Freer, B. R. Fulton, G. Giardina, S. Grévy, D. Guillemaud-Mueller, F. Hanappe, B. Heusch, K. L. Jones, B. Jonson, C. Le Brun, S. Leenhardt, M. Lewitowicz, M. J. Lopez, K. Markenroth, A. C. Mueller, T. Nilsson, A. Ninane, G. Nyman, F. de Oliveira, I. Piqueras, K. Riisager, M. G. Saint Lau-

- rent, F. Sarazin, S. M. Singer, O. Sorlin, and L. Stuttg , Halo structure of ^{14}Be , *Phys. Rev. Lett.* **86**, 600 (2001).
- [26] K. J. Cook, T. Nakamura, Y. Kondo, K. Hagino, K. Ogata, A. T. Saito, N. L. Achouri, T. Aumann, H. Baba, F. Delaunay, Q. Deshayes, P. Doornenbal, N. Fukuda, J. Gibelin, J. W. Hwang, N. Inabe, T. Isobe, D. Kameda, D. Kanno, S. Kim, N. Kobayashi, T. Kobayashi, T. Kubo, S. Leblond, J. Lee, F. M. Marqu s, R. Minakata, T. Motobayashi, K. Muto, T. Murakami, D. Murai, T. Nakashima, N. Nakatsuka, A. Navin, S. Nishi, S. Ogoshi, N. A. Orr, H. Otsu, H. Sato, Y. Satou, Y. Shimizu, H. Suzuki, K. Takahashi, H. Takeda, S. Takeuchi, R. Tanaka, Y. Togano, J. Tsubota, A. G. Tuff, M. Vandebrouck, and K. Yoneda, Halo structure of the neutron-dripline nucleus ^{19}B , *Phys. Rev. Lett.* **124**, 212503 (2020).
- [27] W. Horiuchi and Y. Suzuki, ^{22}C : An s -wave two-neutron halo nucleus, *Phys. Rev. C* **74**, 034311 (2006).
- [28] K. Tanaka, T. Yamaguchi, T. Suzuki, T. Ohtsubo, M. Fukuda, D. Nishimura, M. Takechi, K. Ogata, A. Ozawa, T. Izumikawa, T. Aiba, N. Aoi, H. Baba, Y. Hashizume, K. Inafuku, N. Iwasa, K. Kobayashi, M. Komuro, Y. Kondo, T. Kubo, M. Kurokawa, T. Matsuyama, S. Michimasa, T. Motobayashi, T. Nakabayashi, S. Nakajima, T. Nakamura, H. Sakurai, R. Shinoda, M. Shinohara, H. Suzuki, E. Takeshita, S. Takeuchi, Y. Togano, K. Yamada, T. Yasuno, and M. Yoshitake, Observation of a Large Reaction Cross Section in the Drip-Line Nucleus ^{22}C , *Phys. Rev. Lett.* **104**, 062701 (2010).
- [29] Y. Togano, T. Nakamura, Y. Kondo, J. Tostevin, A. Saito, J. Gibelin, N. Orr, N. Achouri, T. Aumann, H. Baba, F. Delaunay, P. Doornenbal, N. Fukuda, J. Hwang, N. Inabe, T. Isobe, D. Kameda, D. Kanno, S. Kim, N. Kobayashi, T. Kobayashi, T. Kubo, S. Leblond, J. Lee, F. Marqu s, R. Minakata, T. Motobayashi, D. Murai, T. Murakami, K. Muto, T. Nakashima, N. Nakatsuka, A. Navin, S. Nishi, S. Ogoshi, H. Otsu, H. Sato, Y. Satou, Y. Shimizu, H. Suzuki, K. Takahashi, H. Takeda, S. Takeuchi, R. Tanaka, A. Tuff, M. Vandebrouck, and K. Yoneda, Interaction cross section study of the two-neutron halo nucleus ^{22}C , *Phys. Lett. B* **761**, 412 (2016).
- [30] T. Nagahisa and W. Horiuchi, Examination of the ^{22}C radius determination with interaction cross sections, *Phys. Rev. C* **97**, 054614 (2018).
- [31] J. Singh, J. Casal, W. Horiuchi, L. Fortunato, and A. Vitturi, Exploring two-neutron halo formation in the ground state of ^{29}F within a three-body model, *Phys. Rev. C* **101**, 024310 (2020).
- [32] S. Bagchi, R. Kanungo, Y. K. Tanaka, H. Geissel, P. Doornenbal, W. Horiuchi, G. Hagen, T. Suzuki, N. Tsunoda, D. S. Ahn, H. Baba, K. Behr, F. Browne, S. Chen, M. L. Cort s, A. Estrad , N. Fukuda, M. Holl, K. Itahashi, N. Iwasa, G. R. Jansen, W. G. Jiang, S. Kaur, A. O. Macchiavelli, S. Y. Matsumoto, S. Momiyama, I. Murray, T. Nakamura, S. J. Novario, H. J. Ong, T. Otsuka, T. Papenbrock, S. Paschalis, A. Prochazka, C. Scheidenberger, P. Schrock, Y. Shimizu, D. Steppenbeck, H. Sakurai, D. Suzuki, H. Suzuki, M. Takechi, H. Takeda, S. Takeuchi, R. Taniuchi, K. Wimmer, and K. Yoshida, Two-Neutron Halo is Unveiled in ^{29}F , *Phys. Rev. Lett.* **124**, 222504 (2020).
- [33] Z. H. Yang, Y. L. Ye, B. Zhou, H. Baba, R. J. Chen, Y. C. Ge, B. S. Hu, H. Hua, D. X. Jiang, M. Kimura, C. Li, K. A. Li, J. G. Li, Q. T. Li, X. Q. Li, Z. H. Li, J. L. Lou, M. Nishimura, H. Otsu, D. Y. Pang, W. L. Pu, R. Qiao, S. Sakaguchi, H. Sakurai, Y. Satou, Y. Togano, K. Tshoo, H. Wang, S. Wang, K. Wei, J. Xiao, F. R. Xu, X. F. Yang, K. Yoneda, H. B. You, and T. Zheng, Observation of the exotic 0_2^+ cluster state in ^8He , *Phys. Rev. Lett.* **131**, 242501 (2023).
- [34] Y. Yamaguchi, W. Horiuchi, T. Ichikawa, and N. Itagaki, Dineutron-dineutron correlation in ^8He , *Phys. Rev. C* **108**, L011304 (2023).
- [35] J. Tanaka, Z. Yang, S. Typel, S. Adachi, S. Bai, P. van Beek, D. Beaumel, Y. Fujikawa, J. Han, S. Heil, *et al.*, Formation of α clusters in dilute neutron-rich matter, *Science* **371**, 260 (2021).
- [36] L. D. Landau, Electron motion in crystal lattices, *Phys. Z. Sowjet.* **3**, 664 (1933).
- [37] L. Landau and S. Pekar, Effective mass of a polaron, *Zh. Eksp. Teor. Fiz* **18**, 419 (1948).
- [38] C. Baroni, G. Lamporesi, and M. Zaccanti, Quantum mixtures of ultracold atomic gases (2024), [arXiv:2405.14562 \[cond-mat.quant-gas\]](https://arxiv.org/abs/2405.14562).
- [39] E. Nakano, K. Iida, and W. Horiuchi, Quasiparticle properties of a single α particle in cold neutron matter, *Phys. Rev. C* **102**, 055802 (2020).
- [40] H. Moriya, H. Tajima, W. Horiuchi, K. Iida, and E. Nakano, Binding two and three α particles in cold neutron matter, *Phys. Rev. C* **104**, 065801 (2021).
- [41] H. Tajima, H. Moriya, W. Horiuchi, E. Nakano, and K. Iida, Intersections of ultracold atomic polarons and nuclear clusters: how is a chart of nuclides modified in dilute neutron matter?, *AAPPS Bulletin* **34**, 9 (2024).
- [42] H. Tajima, H. Moriya, W. Horiuchi, E. Nakano, and K. Iida, Polaronic proton and diproton clustering in neutron-rich matter, *Phys. Lett. B* **851**, 138567 (2024).
- [43] M.-G. Hu, M. J. Van de Graaff, D. Kedar, J. P. Corson, E. A. Cornell, and D. S. Jin, Bose Polarons in the Strongly Interacting Regime, *Phys. Rev. Lett.* **117**, 055301 (2016).
- [44] N. B. Jorgensen, L. Wacker, K. T. Skalmstang, M. M. Parish, J. Levinsen, R. S. Christensen, G. M. Bruun, and J. J. Arlt, Observation of Attractive and Repulsive Polarons in a Bose-Einstein Condensate, *Phys. Rev. Lett.* **117**, 055302 (2016).
- [45] Z. Z. Yan, Y. Ni, C. Robens, and M. W. Zwierlein, Bose polarons near quantum criticality, *Science* **368**, 190 (2020).
- [46] M. Duda, X.-Y. Chen, A. Schindewolf, R. Bause, J. von Milczewski, R. Schmidt, I. Bloch, and X.-Y. Luo, Transition from a polaronic condensate to a degenerate Fermi gas of heteronuclear molecules, *Nat. Phys.* **19**, 720 (2023).
- [47] S. P. Rath and R. Schmidt, Field-theoretical study of the Bose polaron, *Phys. Rev. A* **88**, 053632 (2013).
- [48] J. Levinsen, M. M. Parish, and G. M. Bruun, Impurity in a Bose-Einstein Condensate and the Efimov Effect, *Phys. Rev. Lett.* **115**, 125302 (2015).
- [49] F. Grusdt, R. Schmidt, Y. E. Shchadilova, and E. Demler, Strong-coupling Bose polarons in a Bose-Einstein condensate, *Phys. Rev. A* **96**, 013607 (2017).
- [50] L. A. Pe a Ardila, N. B. J rgensen, T. Pohl, S. Giorgini, G. M. Bruun, and J. J. Arlt, Analyzing a Bose polaron across resonant interactions,

- Phys. Rev. A **99**, 063607 (2019).
- [51] J. Takahashi, R. Imai, E. Nakano, and K. Iida, Bose polaron in spherical trap potentials: Spatial structure and quantum depletion, *Phys. Rev. A* **100**, 023624 (2019).
 - [52] S. I. Mistakidis, G. C. Katsimiga, G. M. Koutentakis, T. Busch, and P. Schmelcher, Quench Dynamics and Orthogonality Catastrophe of Bose Polarons, *Phys. Rev. Lett.* **122**, 183001 (2019).
 - [53] N.-E. Guenther, P. Massignan, M. Lewenstein, and G. M. Bruun, Bose Polarons at Finite Temperature and Strong Coupling, *Phys. Rev. Lett.* **120**, 050405 (2018).
 - [54] F. Isaule, I. Morera, P. Massignan, and B. Juliá-Díaz, Renormalization-group study of Bose polarons, *Phys. Rev. A* **104**, 023317 (2021).
 - [55] H. Tajima, J. Takahashi, S. I. Mistakidis, E. Nakano, and K. Iida, Polaron problems in ultracold atoms: role of a Fermi sea across different spatial dimensions and quantum fluctuations of a Bose medium, *Atoms* **9**, 18 (2021).
 - [56] F. Scazza, M. Zaccanti, P. Massignan, M. M. Parish, and J. Levinsen, Repulsive fermi and bose polarons in quantum gases, *Atoms* **10**, 55 (2022).
 - [57] E. Wigner, On the Consequences of the Symmetry of the Nuclear Hamiltonian on the Spectroscopy of Nuclei, *Phys. Rev.* **51**, 106 (1937).
 - [58] E. Wigner, On the Structure of Nuclei Beyond Oxygen, *Phys. Rev.* **51**, 947 (1937).
 - [59] T. Mehen, I. W. Stewart, and M. B. Wise, Wigner Symmetry in the Limit of Large Scattering Lengths, *Phys. Rev. Lett.* **83**, 931 (1999).
 - [60] S. Goriely, M. Samyn, P.-H. Heenen, J. M. Pearson, and F. Tondeur, Hartree-Fock mass formulas and extrapolation to new mass data, *Phys. Rev. C* **66**, 024326 (2002).
 - [61] J.-W. Chen, D. Lee, and T. Schaefer, Inequalities for Light Nuclei in the Wigner Symmetry Limit, *Phys. Rev. Lett.* **93**, 242302 (2004).
 - [62] H. Koura, T. Tachibana, M. Uno, and M. Yamada, Nuclidic Mass Formula on a Spherical Basis with an Improved Even-Odd Term, *Prog. Theor. Phys.* **113**, 305 (2005).
 - [63] Z. Li, S. Singh, T. V. Tscherbul, and K. W. Madison, Feshbach resonances in ultracold ^{85}Rb – ^{87}Rb and ^6Li – ^{87}Rb mixtures, *Phys. Rev. A* **78**, 022710 (2008).
 - [64] C.-H. Wu, I. Santiago, J. W. Park, P. Ahmadi, and M. W. Zwierlein, Strongly interacting isotopic Bose-Fermi mixture immersed in a Fermi sea, *Phys. Rev. A* **84**, 011601 (2011).
 - [65] J. W. Park, C.-H. Wu, I. Santiago, T. G. Tiecke, S. Will, P. Ahmadi, and M. W. Zwierlein, Quantum degenerate Bose-Fermi mixture of chemically different atomic species with widely tunable interactions, *Phys. Rev. A* **85**, 051602 (2012).
 - [66] M. Repp, R. Pires, J. Ulmanis, R. Heck, E. D. Kuhnle, M. Weidemüller, and E. Tiemann, Observation of interspecies ^6Li – ^{133}Cs Feshbach resonances, *Phys. Rev. A* **87**, 010701 (2013).
 - [67] M. M. Forbes, A. Gezerlis, K. Hebeler, T. Lesinski, and A. Schwenk, Neutron polaron as a constraint on nuclear density functionals, *Phys. Rev. C* **89**, 041301 (2014).
 - [68] I. Vidaña, Fermi polaron in low-density spin-polarized neutron matter, *Phys. Rev. C* **103**, L052801 (2021).
 - [69] H. Tajima, H. Funaki, Y. Sekino, N. Yasutake, and M. Matsuo, Exploring 3p_0 superfluid in dilute spin-polarized neutron matter, *Phys. Rev. C* **108**, L052802 (2023).
 - [70] J. Levinsen, P. Massignan, F. Chevy, and C. Lobo, p -Wave Polaron, *Phys. Rev. Lett.* **109**, 075302 (2012).
 - [71] Y. Ma and X. Cui, Highly polarized one-dimensional Fermi gases near a narrow p -wave resonance, *Phys. Rev. A* **100**, 062712 (2019).
 - [72] O. I. Utesov and S. V. Andreev, Magnetoroton in a two-dimensional bose-bose mixture, *Phys. Rev. B* **109**, 235135 (2024).
 - [73] M. Matsuo, Spatial structure of neutron Cooper pair in low density uniform matter, *Phys. Rev. C* **73**, 044309 (2006).
 - [74] H. Tajima, H. Moriya, W. Horiuchi, K. Iida, and E. Nakano, Resonance-to-bound transition of ^5He in neutron matter and its analogy with heteronuclear Feshbach molecules, *Phys. Rev. C* **106**, 045807 (2022).
 - [75] K. Nishimura, E. Nakano, K. Iida, H. Tajima, T. Miyakawa, and H. Yabu, Ground state of the polaron in an ultracold dipolar Fermi gas, *Phys. Rev. A* **103**, 033324 (2021).
 - [76] A. Camacho-Guardian, L. A. Peña Ardila, T. Pohl, and G. M. Bruun, Bipolarons in a bose-einstein condensate, *Phys. Rev. Lett.* **121**, 013401 (2018).
 - [77] L. A. P. n. Ardila and S. Giorgini, Impurity in a bose-einstein condensate: Study of the attractive and repulsive branch using quantum monte carlo methods, *Phys. Rev. A* **92**, 033612 (2015).
 - [78] O. I. Utesov, M. I. Baglay, and S. V. Andreev, Effective interactions in a quantum bose-bose mixture, *Phys. Rev. A* **97**, 053617 (2018).
 - [79] W. Li and X. Cui, Repulsive Fermi polarons with negative effective mass, *Phys. Rev. A* **96**, 053609 (2017).
 - [80] J. W. Clark and E. Krotscheck, Alpha matter revisited (2023), [arXiv:2304.08543 \[nucl-th\]](https://arxiv.org/abs/2304.08543).
 - [81] Y. Funaki, H. Horiuchi, W. von Oertzen, G. Röpke, P. Schuck, A. Tohsaki, and T. Yamada, Concepts of nuclear α -particle condensation, *Phys. Rev. C* **80**, 064326 (2009).
 - [82] P. van Wyk, H. Tajima, D. Inotani, A. Ohnishi, and Y. Ohashi, Superfluid Fermi atomic gas as a quantum simulator for the study of the neutron-star equation of state in the low-density region, *Phys. Rev. A* **97**, 013601 (2018).
 - [83] N. Itagaki and S. Okabe, Molecular orbital structures in ^{10}Be , *Phys. Rev. C* **61**, 044306 (2000).
 - [84] M. Dan, R. Chatterjee, and M. Kimura, A description of the structure and electromagnetic breakup of ^{11}Be with microscopic inputs, *Eur. Phys. J. A* **57**, 203 (2021).
 - [85] P. Van Isacker, D. D. Warner, and D. S. Brenner, Test of Wigner's Spin-Isospin Symmetry from Double Binding Energy Differences, *Phys. Rev. Lett.* **74**, 4607 (1995).
 - [86] W. Satuła, D. J. Dean, J. Gary, S. Mizutori, and W. Nazarewicz, On the origin of the Wigner energy, *Phys. Lett. B* **407**, 103 (1997).
 - [87] N. Zeldes, The physical origin of the Wigner term and its persistence in heavy nuclei, *Phys. Lett. B* **429**, 20 (1998).
 - [88] R. R. Chasman, n - p Pairing—diagonal matrix elements: Wigner energy, symmetry energy and spectroscopy, *Phys. Lett. B* **577**, 47 (2003).
 - [89] R. R. Chasman, n - p Pairing, Wigner Energy, and Shell Gaps, *Phys. Rev. Lett.* **99**, 082501 (2007).
 - [90] M. W. Kirson, Global systematics of the Wigner energy, *Phys. Lett. B* **661**, 246 (2008).

- [91] K. Neergård, Pairing theory of the symmetry energy, *Phys. Rev. C* **80**, 044313 (2009).
- [92] I. Bentley and S. Frauendorf, Relation between Wigner energy and proton-neutron pairing, *Phys. Rev. C* **88**, 014322 (2013).
- [93] D. Negrea and N. Sandulescu, Isovector proton-neutron pairing and Wigner energy in Hartree-Fock mean field calculations, *Phys. Rev. C* **90**, 024322 (2014).
- [94] L. Pitaevskii and S. Stringari, *Bose-Einstein condensation and superfluidity*, Vol. 164 (Oxford University Press, 2016).
- [95] J. W. Clark and E. Krotscheck, α -cluster matter reexamined, *Phys. Rev. C* **109**, 034315 (2024).
- [96] H. Koura, M. Uno, T. Tachibana, and M. Yamada, Nuclear mass formula with shell energies calculated by a new method, *Nucl. Phys. A* **674**, 47 (2000).
- [97] M. Takano and M. Yamada, Variational study of asymmetric nuclear matter and a new term in the mass formula, *Prog. Theor. Phys.* **116**, 545 (2006).
- [98] P. Naidon, Two impurities in a bose-einstein condensate: From yukawa to efimov attracted polarons, *J. Phys. Soc. Jpn.* **87**, 043002 (2018).
- [99] G. Panochko and V. Pastukhov, Two- and three-body effective potentials between impurities in ideal BEC, *J. Phys. A: Math. Theor.* **54**, 085001 (2021).
- [100] K. Fujii, M. Hongo, and T. Enss, Universal van der Waals Force between Heavy Polarons in Superfluids, *Phys. Rev. Lett.* **129**, 233401 (2022).
- [101] R. Paredes, G. Bruun, and A. Camacho-Guardian, Perspective: Interactions mediated by atoms, photons, electrons, and excitons (2024), [arXiv:2406.13795 \[cond-mat.quant-gas\]](https://arxiv.org/abs/2406.13795).
- [102] E. Nakano, T. Miyakawa, and H. Yabu, Two-body problem of impurity atoms in dipolar fermi gas, *arXiv preprint arXiv:2404.14866* (2024).
- [103] G. Röpke, A. Schnell, P. Schuck, and P. Nozières, Four-Particle Condensate in Strongly Coupled Fermion Systems, *Phys. Rev. Lett.* **80**, 3177 (1998).
- [104] N. Sandulescu, D. Negrea, J. Dukelsky, and C. W. Johnson, Quartet condensation and isovector pairing correlations in $N = Z$ nuclei, *Phys. Rev. C* **85**, 061303 (2012).
- [105] R. Sen'kov and V. Zelevinsky, Unified BCS-like model of pairing and alpha-correlations, *Phys. At. Nucl.* **74**, 1267 (2011).
- [106] N. Sandulescu, D. Negrea, and D. Gambacurta, Proton-neutron pairing in $N = Z$ nuclei: Quartetting versus pair condensation, *Phys. Lett. B* **751**, 348 (2015).
- [107] V. Baran and D. Delion, A quartet BCS-like theory, *Phys. Lett. B* **805**, 135462 (2020).
- [108] Y. Guo, H. Tajima, and H. Liang, Cooper quartet correlations in infinite symmetric nuclear matter, *Phys. Rev. C* **105**, 024317 (2022).